

R.J. Cameron

European Space Research and Technology Centre, Noordwijk, The Netherlands

and J.D. Rhodes

Department of Electrical and Electronic Engineering, University of Leeds, Leeds, England

Summary

Two realisations are discussed for dual mode in-line bandpass microwave filters which have asymmetrically-valued couplings about the physical centre of the filter. Advantages are gained in the first type of realisation which has no realisability conditions on the pattern of the transmission zeros in the complex-plane representation of the transfer function, and in the second which needs less coupling elements.

Introduction

The most common method for realising a rational transfer function in waveguide is to first synthesise a cross-coupled double array prototype network¹ (fig. 1).

The network is a folded ladder network of admittance inverters K_i and shunt capacitors C_i cross coupled by further inverters K_j . Fig. 1b shows the corresponding coupling and routing diagram for this network, where the capacitors are depicted as nodes intercoupled by forward- and cross-couplings M_{ij} . Fig. 1c gives the coupling matrix for this generalised cross-coupled network together with the formulae used to generate the elements of the matrix from the elements of the network. The procedure is equivalent to scaling the internal capacitors of the network to unity.

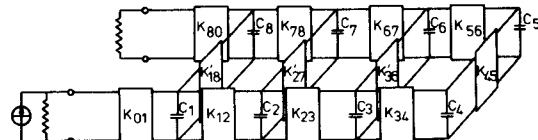


Fig. 1. Cross coupled double array prototype network

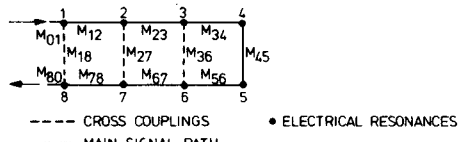


Fig. 1b. Coupling and routing diagram

1	2	3	4	5	6	7	8	
M_{01}	M_{12}	M_{23}	M_{34}	M_{45}				
M_{01}	M_{18}	M_{27}	M_{36}	M_{45}				
	M_{01}	M_{78}	M_{67}	M_{56}				

for forward couplings

$$M_{i,i+1} = \frac{K_{i,i+1}}{\sqrt{C_i \cdot C_{i+1}}} \quad \begin{cases} i = 0 \rightarrow N \\ N = \text{order of filter} \\ C_0 = C_{N+1} = 1 \end{cases}$$

for cross couplings

$$M_{j,N-i+1} = \frac{K'_{j,N-i+1}}{\sqrt{C_j \cdot C_{N-i+1}}} \quad \begin{cases} j = 1 \rightarrow n-1 \\ n = N/2 \end{cases}$$

Fig. 1c. Coupling matrix and formulae

A dual mode filter may then be directly synthesised from this coupling matrix. An 8th order example is shown in fig. 2 where the coupling elements are realised by slots or screws.

The structure has two major shortcomings; the ingoing and outgoing orthogonally polarised signals will have to be separated, probably with an orthomode transducer, and there is an isolation problem due to the input and output coupling irises being in the

same physical cavity.

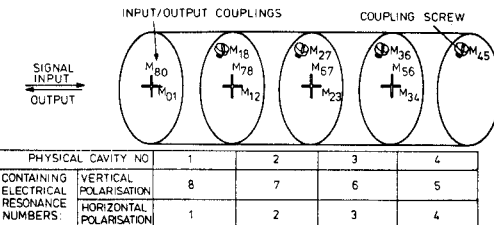


Fig. 2. 8th degree reflective dual mode filter

A solution to both these problems is to rotate the coupling matrix with similarity transformations until only those couplings exist that may be realised with the available coupling devices of an 'in-line' or 'propagating' dual mode structure (fig. 3). This reconfiguration procedure used to be achieved by computer-aided optimisation but more recently analytic methods have been derived for even-degree characteristics 6-12 inclusive. Attached to the formulae for these realisations are conditions related to the locations of the transmission zeros of the transfer function in the complex plane.

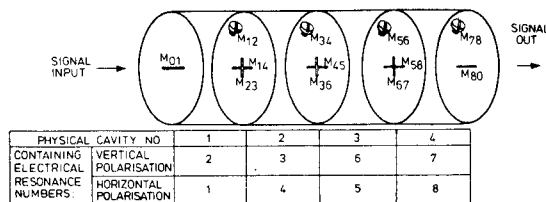


Fig. 3. 8th degree in-line dual mode filter

These realisability conditions were first encountered when attempting to realise with an in-line symmetric structure, an 8th degree transfer characteristic with a j -axis zero pair for an attenuation pole pair and a real-axis zero pair for group delay self-equalisation. The realisability conditions were violated, and this prompted a study into the realisations of characteristics with asymmetrically-valued coupling elements, and the result was two different types of 'in-line' asymmetric structure:

- the general asymmetric (GA) in-line structure
- and ii) the cascade quadruplet (CQ) in-line structure.

The GA structure is so called because there are no singularity-pattern-related realisability conditions attached to the realisation process. The CQ structure has alternate single-slot and cruciform-slot internal irises along the length of the filter, thereby reducing the number that have to be manufactured. The CQ structure does have realisation conditions but these appear to be different to those for the equivalently-ordered symmetric structure. Both CQ and GA structures are able to realise electrically asymmetric characteristics, such as single-ended filters for multiplexer applications.

Coupling Matrix Reconfiguration

As with the symmetric-structure in-line realisation process a series of j similarity transformations are applied to the coupling matrix. For the r th rotation:

$$M_r = R_r \cdot M_{r-1} \cdot R_r^T$$

$$r = 1, 2, 3 \dots j$$

where M_r is the coupling matrix resultant from the r th rotation, M_0 is the original cross-coupled double array coupling matrix (fig. 1c) and R is the rotation matrix as defined in fig. 4. R^T is the transpose of R

	1	2	3	4	5	6	7	8	
1	1								
2		c				s			
3			1						
4				1					
5					1				
6						c			
7							1		
8								1	

for pivot [m,n]

$$R_{mm} = R_{nn} = \cos \theta$$

$$R_{mn} = -R_{nm} = \sin \theta$$

$$c = \cos \theta \quad s = \sin \theta$$

Figure 4. Example of an 8×8 rotation matrix, pivot [2,6], angle θ

The aim of the procedure is to apply a series of similarity transformations to the coupling matrix, starting with the cross-coupled double array coupling matrix (M_0), and ending up after the final (j th) rotation with a coupling matrix (M_j), whose finite elements correspond to the available coupling devices within an in-line asymmetric structure.

General Asymmetric Structure

Table I is a list of the pivots and rotation angles to be applied in order, to obtain asymmetric in-line structures for dual mode filters of (even) degrees 6 to 14 inclusive. The angle θ_r of each rotation is derived from the formula shown in Table I, using the matrix elements from the coupling matrix resultant from the previous rotation

Order N	Rotation No. r	Pivot [i,j]	$\theta_r = \tan^{-1}(k \cdot M_{u1,u2}/M_{v1,v2})$				
			u1	u2	v1	v2	k
6	1	[2, 4]	2	5	4	5	+1
8	1	[4, 6]	3	6	3	4	-1
	2	[2, 4]	2	7	4	7	+1
	3	[3, 5]	2	5	2	3	-1
	4	[5, 7]	4	7	4	5	-1
10	1	[4, 6]	4	7	6	7	+1
	2	[6, 8]	3	8	3	6	-1
	3	[7, 9]	6	9	6	7	-1
12	1	[5, 9]	4	9	4	5	-1
	2	[3, 5]	3	10	5	10	+1
	3	[2, 4]	2	5	4	5	+1
	4	[6, 8]	3	8	3	6	-1
	5	[7, 9]	6	9	6	7	-1
	6	[8, 10]	5	10	5	8	-1
	7	[9, 11]	8	11	8	9	-1
14	1	[6, 10]	5	10	5	6	-1
	2	[4, 6]	4	11	6	11	+1
	3	[7, 9]	4	9	4	7	-1
	4	[8, 10]	7	10	7	8	-1
	5	[9, 11]	6	11	6	9	-1
	6	[10, 12]	9	12	9	10	-1
	7	[5, 7]	4	7	4	5	-1
	8	[7, 9]	6	9	6	7	-1
	9	[9, 11]	8	11	8	9	-1
	10	[11, 13]	10	13	10	11	-1

Table I. Pivotal positions and rotation angles for general asymmetric in-line realisations, orders 6(2) 14.

A 14th degree linear phase laboratory model (fig. 5) was constructed and measured using the GA realisation procedure. Centre frequency is 11.575 GHz and bandwidth 80 MHz, and the measured amplitude and group delay responses are shown in figs 6 and 7.

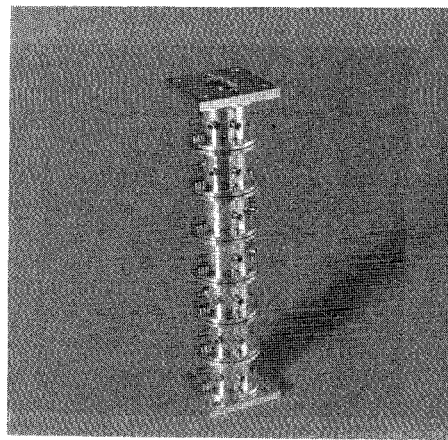


Fig. 5. 14th degree linear phase filter - GA structure

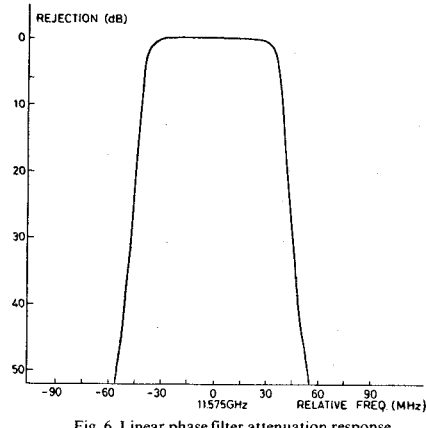


Fig. 6. Linear phase filter attenuation response

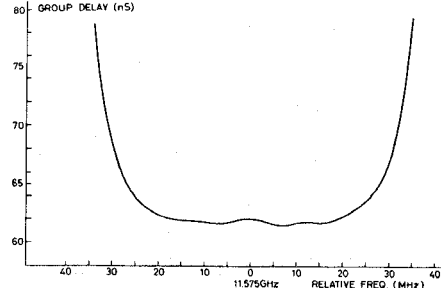


Fig. 7. Linear phase filter group delay response

Cascade Quadruplet Structure, Degrees 6, 8 and 10

The 6th degree CQ structure is in fact the same as the 6th degree GA structure, and further analysis is unnecessary. The 8th degree is however a good deal more complex to analyse but explicit formulae are given in fig. 8 for converting the couplings of the original double-array matrix into those for the CQ matrix. The 10th degree case uses the same formulae as the 8th degree case, but two preliminary rotations are required, as defined in Table II.

Rotation no. r	Pivot [i,j]	$\theta_r = \tan^{-1}(+ M_{u1,u2}/M_{v1,v2})$			
		u1	u2	v1	v2
1	[3,7]	3	8	7	8
2	[4,6]	4	7	6	7

Table II. 10th order preliminary rotations

	1	2	3	4	5	6	7	8
1		M_{12}^{IV}		M_{14}^{IV}				
2	M_{12}^{IV}		M_{23}^{IV}					
3		M_{23}^{IV}		M_{34}^{IV}				
4		M_{34}^{IV}		M_{35}^{IV}				
5			M_{35}^{IV}	M_{36}^{IV}		M_{58}^{IV}		
6				M_{58}^{IV}	M_{57}^{IV}	M_{56}^{IV}		
7					M_{57}^{IV}	M_{58}^{IV}		
8					M_{58}^{IV}	M_{56}^{IV}		

Fig. 8a. 8th order CQ coupling matrix

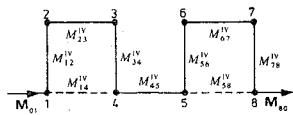


Fig. 8b. 8th order CQ coupling and routing diagram

$$M_{12}^{IV} = c_4 M_{12} \quad M_{23}^{IV} = c_1 c_4 \left[M_{23} - \frac{t_4}{c_2} (M_{34} - t_1 M_{45}) \right]$$

$$M_{78}^{IV} = c_3 M_{78} \quad M_{34}^{IV} = c_1 c_4 \left[t_4 M_{23} + \frac{1}{c_2} (M_{34} - t_1 M_{45}) \right]$$

$$M_{14}^{IV} = s_4 M_{12} \quad M_{45}^{IV} = \frac{-M_{27}}{s_3 s_4}$$

$$M_{58}^{IV} = -s_4 M_{78} \quad M_{56}^{IV} = c_2 c_3 \left[\frac{1}{c_1} (M_{56} + t_2 M_{45}) - t_3 M_{67} \right]$$

$$M_{67}^{IV} = c_2 c_3 \left[\frac{t_3}{c_1} (M_{56} + t_2 M_{45}) + M_{67} \right]$$

where t_i is the solution of the quadratic equation:

$$t_1^2 (M_{27} M_{45} M_{34} - M_{36} M_{67} M_{23} + M_{36} M_{56} M_{27})$$

$$+ t_1 (M_{23} M_{67} M_{36} - M_{27} (M_{36}^2 - M_{56}^2 - M_{45}^2 + M_{34}^2))$$

$$- M_{27} (M_{56} M_{36} + M_{34} M_{45}) = 0$$

$$\text{and } t_2 = - \left[\frac{M_{36} - t_1 M_{56}}{M_{34} - t_1 M_{45}} \right] \quad t_3 = \frac{-M_{27}}{s_1 M_{23}} \quad t_4 = \frac{-M_{27}}{s_2 M_{67}}$$

Fig. 8c. 8th order CQ coupling formulae

$$t_3 = \tan \theta_3 \quad c_1 = \cos \theta_1 \text{ etc}$$

An 8th degree laboratory model (fig. 9) was also constructed and measured. The prototype transfer function had a real-axis zero pair for group delay equalisation, and a j-axis zero pair for attenuation poles. This singularity pattern violates the realisation conditions for the symmetric structure. Centre frequency is 11.550 GHz, BW 120 MHz and the amplitude and group delay responses are shown in figs 10 and 11.

Conclusion

Procedures have been presented for the synthesis of two types of asymmetric dual mode bandpass filters. These procedures are very easy to program, and consume negligible amounts of computer time. A laboratory model has been constructed in each type of realisation using transfer characteristics unrealisable with a symmetric structure.

References

1. Rhodes J D 1970, A low pass prototype network for microwave linear phase filters, IEEE MTT-18 June, pp 290-300.

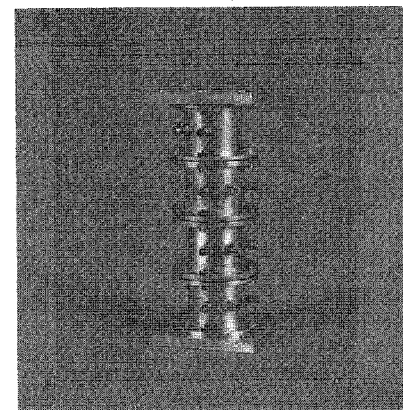


Fig. 9. 8th order pseudo-elliptic self-equalised filter - CQ structure

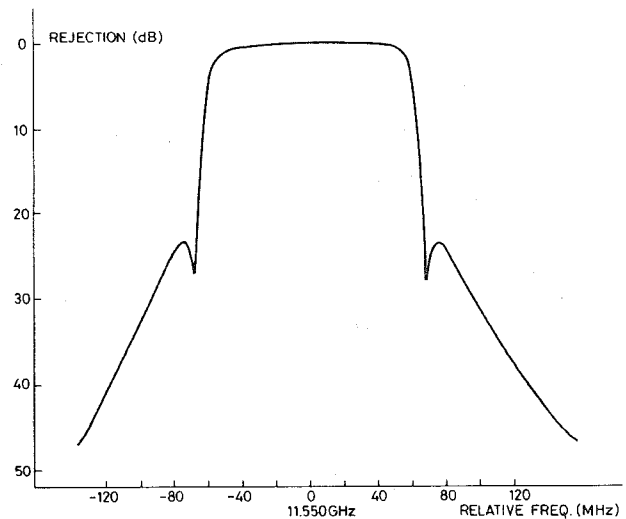


Fig. 10. CQ filter attenuation response

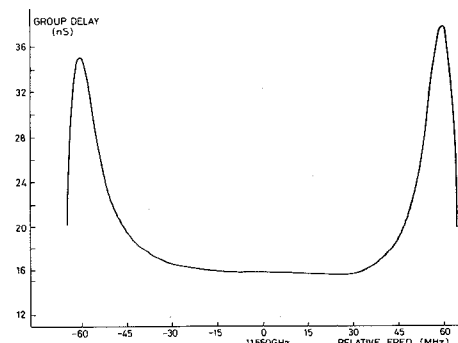


Fig. 11. CQ filter group delay response